Cyclophane $5H_2$ was prepared from $5H^+$ and BNAH as described for $1H_2$ in 78% yield. ^1H NMR $CDCl_3$) δ 1.95 ($ArCH_3$), 2.36 ($ArCH_3$), 2.48 ($C(4)H_B$), 2.56 ($C(4)H_A$), 2.8–4.2 (CH_2CH_2), 3.82 (OCH_3), 4.60 (CH_2Ph), 5.41 (NH), 6.62 (Ar H), 7.30 (C(2)H, C(6)H), 7.35 (PhH).

(3.6) Deuterium Incorporation. The monodeuterated compounds nHD (n = 3–6) were prepared by reaction of the appropriate pyridinium ion (nH^+) with an equimolar amount of BNAH-4-d_2. For n = 4–6 the same reaction conditions were applied as described above for the conversion $1H^+ \rightarrow 1H_2$. Under these conditions formation of **3HD** gave no satisfactory results. In this case the reaction was performed at 20 °C during 4 days (yield 64%).

(3.7) Oxidation of nHD by AcH^+. Compounds **4HD**, **5HD**, and **6HD** were subjected to oxidation by AcH^+ and the deuterium content of the 10-methylacridan thus obtained was determined by MS (field-ionization technique). To avoid isotopic exchange[23] between acridan and unreacted AcH^+ the reactions were carried out with a twofold excess of nHD. Typically solutions of nHD (0.6 mmol) and AcH^+ (0.3 mmol) in dimethyl sulfoxide (2 mL each) were mixed and stirred for 1 h at 20 °C. The reaction mixture was than poured in ice water and the white precipitate of 10-methylacridan collected by filtration and purified by recrystallization from ethanol/water 2:1.

Determination of the deuterium content was performed by MS using the field-ionization (FI) technique as described extensively before.[22] MS-FI was found[22] to avoid the problem of erratic M/M + 1 ratios, which thwarts MS measurements on 10-methylacridan under electron-impact conditions. All MS-FI measurements were repeated at least 5 times. The following peak ratios m/z 195/196/197 were observed in the molecular ion region: 55.4/100/22.1 for the product from reaction of AcH^+ with **4HD** and 56.1/100/23 from the reaction with **5HD**. The reference experiment with **6HD** gave a ratio 100/38.5/4.5 while unlabeled AcH_2 gave 100/21.1/zero.

(3.8) Kinetic Procedures. The rate of reduction of nH^+ was studied with β-NADH (Merck) as a reductant in aqueous solution at 20 °C. In all cases the reduction product nH_2 absorbs at longer wavelength (see Table II) than **NADH** (λ_{max} = 340 nm, ϵ = 6220 L mol^{-1} cm^{-1}), which allowed the reaction to be followed by monitoring the increase of absorption at a wavelength (λ > 400 nm) where the absorption of NADH may be neglected.

For the reactive systems (n = **4**, **5**, **6**) the reactions were carried out under second-order conditions with equal initial concentrations of NADH and nH^+ (both $\sim 10^{-4}$ mol L^{-1}). For the less reactive systems the reaction is unduly slow at these concentrations and the spontaneous decomposition of NADH (mainly by hydratation) becomes competitive. Therefore a tenfold excess of nH^+ ($\sim 10^{-3}$ mol L^{-1}) was employed for n = **1**, **2**, and **3**. In all cases isosbestic points were observed over at least two **NADH** half-lifetimes and linear second order (n = **4**, **5**, **6**) and pseudofirst-order (n = **1**, **2**, **3**) kinetic plots were obtained. Results are compiled in Table III. The rate of oxidation of nH_2 was studied with AcH^+ as an oxidant in acetonitrile at 20 °C. All reactions were measured under pseudo-first-order conditions with initial concentrations $nH_2 \approx 10^{-3}$ mol L^{-1} and $AcH^+ \approx 10^{-5}$ mol L^{-1}. The decrease of the AcH^+ concentration is very conveniently monitored by fluorescence spectroscopy. Selective excitation of AcH^+ was achieved at 450 nm. The strong green fluorescence (quantum yield near unity) occurs at 500 nm. Results are compiled in Table III.

Acknowledgment. We thank C. H. Stam (University of Amsterdam, Laboratory for Crystallography) for performance and discussion of the X-ray structure determinations. Measurement of the 360-MHz ^1H NMR spectra by R. Kaptein and K. Dijkstra (University of Groningen) is gratefully acknowledged. We thank C. Kruk et al. for extensive 250-MHz ^1H NMR and NOE measurements. FI-MS measurements were realized by the courtesy of N. M. M. Nibbering, R. H. Fokkens, and J. J. Zwinselman. We thank U. K. Pandit for stimulating discussions on the reactivity of NAD(H) models. The 360-MHz ^1H NMR facilities were made available- and part of these investigations was supported by the Netherlands Foundation for Chemical Research (SON) with financial aid from the Netherlands Organization for the Advancement of Pure Research (ZWO).

Resonant Fluorescence Study of the Eu^{3+}-Substituted Ca^{2+} Site in Busycon Hemocyanin: Structural Coupling between the Heterotropic Allosteric Effector and the Coupled Binuclear Copper Active Site

Yeong Tsyr Hwang,[†] Leonard J. Andrews,*[‡] and Edward I. Solomon*[†]

Contribution from the Department of Chemistry, Stanford University, Stanford, California 94305, and GTE Laboratories, Waltham, Massachusetts 02254.
Received September 12, 1983

Abstract: Eu^{3+} was substituted for Ca^{2+} as an allosteric effector in hemocyanin, and its laser-induced f–f fluorescence was studied to probe the allosteric effects on the Ca^{2+} binding site induced by deoxygenation of the binuclear copper active site. The $^7F_0 \rightarrow {}^5D_0$ excitation spectrum of Eu^{3+} was monitored to define two kinds of high-affinity Eu^{3+} binding sites in the hemocyanin biopolymer, one of which is competitive with the Ca^{2+} ion. The fluorescence decay lifetimes of this Ca^{2+}-competitive Eu^{3+} site were measured in D_2O and H_2O buffer which permitted an estimate of the coordinated water number at the Eu^{3+} ion. The results show that in the relaxed quaternary structure the Ca^{2+} site is located in a very hydrophilic environment with $\sim$5 H_2O molecules and $\sim$3 protein ligands in its first coordination sphere. When the coupled binuclear copper active site is deoxygenated, the Ca^{2+} site appears to release one coordinated water molecule upon binding an additional protein ligand. This may correlate to the allosteric role of Ca^{2+} in stabilizing the tense quaternary structure. Further, the internal energy transfer from the Eu^{3+} allosteric site to the coupled binuclear copper active site was monitored (using the met active site derivative) and used to estimate the average distance between these two sites to be $\sim$32 Å.

Under physiological conditions, mollusc hemocyanins are present as highly aggregated biopolymers with a molecular architecture composed of 20 subunits. Each subunit contains eight binuclear copper active sites covalently linked in a single polypeptide chain of about 400 000 daltons. Hemocyanin functions as an oxygen-carrying protein with a Cu:dioxygen ratio of 2:1. Oxygen binds as peroxide bridging two cupric ions, producing intense blue color with strong absorption in the regions of 345 and 570 nm,[1] corresponding to peroxide-to-copper(II) charge-

[†] Stanford University.
[‡] GTE Laboratories.

0002-7863/84/1506-3832$01.50/0

transfer transitions. When oxygen is removed from the active site, producing the deoxy form, the absorbances at 345 and 570 nm are eliminated, leaving both Cu atoms in the Cu(I) oxidation state. Along with oxy and deoxyhemocyanin sites, an additional active site derivative has been prepared.[2] Methemocyanin can be generated by associative ligand displacement of peroxide from the oxy active site leaving the binuclear copper in the cupric state, but eliminating the $O_2^{2-} \rightarrow$ Cu charge-transfer (CT) transitions. Also of interest to this study is the half-met derivative where the binuclear copper active site has been oxidized by one electron to the EPR-detectable mixed-valent Cu(II)Cu(I) state.

The reversible oxygen binding of hemocyanin is characterized by cooperativity which can be explained in terms of two limiting conformational states, the tense (deoxygenated) state and the relaxed (oxygenated) state.[3,4] The equilibrium between these two quaternary structures is regulated by "homotropic effectors" (O_2) and "heterotropic effectors" (Ca^{2+}, H^+).[5,6] In order to study the role exerted by these allosteric effectors, a Spectral Probe hemocyanin biopolymer has been prepared,[7] in which a small fraction (10 to 15%) of EPR-detectable half-met sites are dispersed among the EPR-nondetectable oxy-active sites. Detailed chemical and spectroscopic studies of this Spectral Probe hemocyanin derivative enable us to evaluate the effects on the active site of change in quaternary structure induced by deoxygenation of the majority of oxy sites (homotropic effect). In addition, the heterotropic effector, Ca^{2+}, was found to be capable of inducing interactions among copper active sites by stabilizing the tense quaternary structure.[8a] In spite of this important ability of Ca^{2+} to induce cooperativity in oxygen binding, detailed structural information on this binding site still remains to be elucidated.

As Ca^{2+} lacks suitable open-shell spectroscopic properties, it cannot be studied by most conventional physical methods. Fortunately, however, lanthanide ions possess chemical and open f shell spectral properties which make them excellent probes for Ca^{2+}.[10] In forming complexes, both Ca^{2+} and Ln^{3+} prefer oxygen- to nitrogen-donor ligands. In protein systems, the preferential ligands appear to be RCO_2^-, RO^-, C=O, and H_2O. These ions display a variable coordination number and lack strong directionality in binding donor groups.[11] In addition, the lanthanide ions span a series of ionic radii similar to those of Ca^{2+} in various coordination numbers.[12] In this study, the $4f^6$ lanthanide ion Eu^{3+}, which possesses an ionic radius close to that of Ca^{2+} in an environment of one less coordination number, was used to probe the Ca^{2+} binding site in hemocyanin. As Eu^{3+} usually exhibits coordination numbers of 8 to 10 whereas Ca^{2+} is more often 7 to 9, we may anticipate a small decrease in ionic radius or increase in coordination number upon Eu^{3+} replacement of Ca^{2+} in the protein. The unit charge difference between Ca^{2+} and Eu^{3+} is expected to be of secondary importance to the substitution, as evidenced in several biological systems wherein cations with comparable radii but which differ by a single charge unit are competitive for the same site.[13]

Since the f–f intraconfiguration transitions in rare earth ions are Laporte forbidden, the Ln^{3+} ion exhibits an absorption spectrum with a typical molar absorptivity on the order of 1 $M^{-1}cm^{-1}$. When the ion is solvated or bound to the protein, the forbidden nature of these transitions is overcome by increasing the degree of asymmetry in the local environment of the Ln^{3+}. Nevertheless, the Ln^{3+}-protein absorption is still difficult to observe because the protein concentration is limited to about 1 mM. Fortunately, however, the f–f fluorescence provides an excellent means of studying the properties of the Ln^{3+} in the protein. Due to the weak absorptivity of the Ln^{3+} ion, excitation of the Ln^{3+} emission has to be accomplished either by direct excitation of the metal ion chromophore with a powerful excitation source or by an indirect mechanism involving optical excitation of the protein aromatic chromophores followed by radiationless energy transfer to the Ln^{3+} ion. Direct excitation of Eu^{3+} using a pulsed laser source has been employed recently in the study of luminescence lifetimes for a variety of complexes in aqueous solution,[14] where the fluorescence decay lifetimes of Eu^{3+} have been measured as a function of D_2O content of the solvating water molecules.[15,16] The correlation generated by these studies allows one to estimate the number of water molecules bound to Eu^{3+} in an unknown complex. We report here the use of this method to evaluate the changes in the Ca^{2+} allosteric site which correlate to changes in protein conformation with cooperative oxygen binding. We further evaluate the internal energy transfer in Eu^{3+}–oxyhemocyanin and use this to estimate the average distance between the allosteric Ca^{2+} sites and the coupled binuclear copper-active sites.

Materials and Methods

A. Sample Preparation. $EuCl_3 \cdot 6H_2O$ was obtained from Aldrich Chemical Co. and deuterium oxide (99.8%) from Merck Isotopes. During the course of the titration, the concentrations of Ca^{2+} and Eu^{3+} were not greater than 0.5 and 0.01 M, respectively. At these concentrations, the H_2O in $CaCl_2 \cdot 2H_2O$ and $EuCl_3 \cdot 6H_2O$ hydrated salts contributes less than 0.2% of the total water in the final deuterated solution. $EuCl_3 \cdot 6H_2O$ and $CaCl_2 \cdot 2H_2O$ were directly dissolved into D_2O and H_2O, separately, to make 1 M stock solutions which were then added to the hemocyanin solution by microsyringe. Deuterated Tris buffer was prepared from pH 7.0, 0.05 M Tris/H_2O solution by evaporating almost to dryness and then adding D_2O. This evaporation–dilution cycle was repeated at least three times to completely deuterate exchangeable protons.

Busycon canaliculatum was prepared as described[7] and dialyzed against pH 7.0, 0.05 M Tris/HCl buffer. Methemocyanin was prepared by incubation of oxyhemocyanin at 37 °C for 48 h in pH 5.0, 0.1 M sodium acetate buffer with 100-fold excess NaF then dialyzed into pH 7.0, 0.05 M Tris buffer. For the preparation of deuterated oxy- and methemocyanin solutions, the oxy- and met-hemocyanin H_2O-containing solutions were centrifuged at 48 000 × g for 5 h to separate the hemocyanin as a pellet. This pellet was dissolved in deuterated Tris buffer and again centrifuged and redissolved in deuterated Tris buffer to yield a 0.5 mM protein solution. Most of the lifetime measurements were performed on 0.075 mM hemocyanin, prepared by diluting the 0.5 mM protein with D_2O, as Tris is capable of forming complexes with Eu^{3+} at high concentrations. Spectral Probe hemocyanin derivatives were prepared as reported in our previous work.[17]

B. Instrumentation. Eu^{3+} excitation spectra were recorded with use of a Lambda Physics N_2-Rhodamine 6G dye laser (50 Hz, 0.06-nm spectral width, 0.25 mJ, 5-ns pulse duration) to pump the $\Delta J = 0$ transition near 579 nm and a Coumarin 460 to pump $\Delta J = 2$ transition near 465 nm. The dye laser beam was aligned adjacent to the emitting side of a 1 × 1-cm square optical cuvette (to eliminate interference from self-absorption), and an $f/2$ lens oriented perpendicular to the beam focused the Eu^{3+} luminescence onto a RCA 4832 GaAs photomultiplier. The emission was isolated from the pump radiation by an interference

(1) Eickman, N. C.; Himmelwright, R. S.; Solomon, E. I. *Proc. Natl. Acad. Sci. U.S.A.* **1979**, *76*, 2094.
(2) Solomon, E. I. In "Copper Proteins"; Spiro, T. G., Ed.; Wiley-Interscience: New York, 1981; p 41.
(3) Van Holde, K. E.; Miller, K. *Biochemistry* **1974**, *13*, 1668.
(4) Brouwer, M.; Bonaventura, C.; Bonaventura, J. *Biochemistry* **1978**, *17*, 2148.
(5) Lamy, J.; Lamy, J., Eds., "Invertebrate Oxygen-Binding Proteins"; Dekker: New York, 1981.
(6) Van Holde, K. E.; Van Bruggen, E. F. J. In "Subunits in Biological Systems"; Timasheff, S. N., Freeman, G. D., Eds.; Dekker: New York, 1971; Vol. 5, pp 1–53.
(7) Hwang, Y. T.; Solomon, E. I. *Proc. Natl. Acad. Sci. U.S.A.* **1982**, *79*, 2564.
(8) (a) In fact, Ca^{2+} not only plays a role in enhancing cooperative oxygen binding but also promotes about 20% of the hemocyanin molecules to associate beyond the "whole molecule" (which predominates at physiological conditions).[8b] Although the correlation between the shift of aggregation state and the cooperative oxygen binding has not yet been well defined, the Spectral Probe hemocyanin results have demonstrated that the site–site interactions arise mainly within a subunit.[9] Thus, Ca^{2+} appears to have its regulatory role in oxygen binding independent of its effect on protein aggregation. (b) Loeffler, M. C.; Su, S. S.; Li, N. *Bioinorg. Chem.* **1978**, *8*, 133.
(9) Hwang, Y. T.; Solomon, E. I., to be published.
(10) Nieboer, E. *Coord. Chem. Rev.* **1975**, *22*, 1.
(11) Martin, R. B.; Richardson, F. S. *Q. Rev. Biophys.* **1979**, *12*, 181.
(12) Shannon, R. D. *Acta Crystallogr., Sect. A* **1976**, *A32*, 751.
(13) Hermsmeyer, K.; Sperelakis, N. *Am. J. Physiol.* **1970**, *219*, 1108.
(14) Horrocks, W. Dew, Jr.; Sudnick, D. R *Acc. Chem. Res.* **1981**, *14*, 384.
(15) Horrocks, W. Dew, Jr.; Schmidt, G. F.; Sudnick, D. R.; Kittrell, C.; Bernheim, R. A. *J. Am. Chem. Soc.* **1977**, *99*, 2378.
(16) Horrocks, W. Dew, Jr.; Sudnick, D. R. *J. Am. Chem. Soc.* **1979**, *101*, 334.

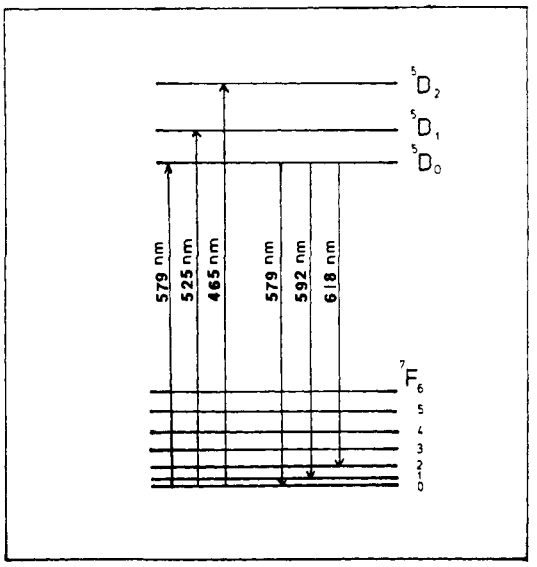

Figure 1. The two lowest-energy multiplets of the Eu^{3+} $4f^6$ electronic configuration.

filter and a Corning 2-52 cutoff filter. This enabled the $^5D_0 \rightarrow {}^7F_2$ transition to be principally monitored. The output of the photomultiplier was fed into a PAR 162 boxcar integrator (10 kΩ input) equipped with a Model 165 base line sampling plug-in. The boxcar aperture was set to 200 μs and was delayed 50 μs after laser firing to avoid scattered dye fluorescence. The output of the boxcar was recorded with a Nicolet 1170 signal averager using a 12 bit A/D converter. Wavelength synchronization between the Nicolet and the dye laser was accomplished with an interface on the dye laser driver which provided a TTL pulse for the Nicolet address advance. While multiple scans for signal averaging could be performed, the S/N of the system was sufficiently good that this option was exercised only in experiments using the lowest Eu^{3+} concentration (0.03 mM).

The dye laser wavelength and spectral width were determined by using a 0.5-m Jarrell-Ash spectrometer as a narrow band detector (resolution 0.025 nm). The spectrometer was set to the peak of the 579.065-nm line from a low-pressure Hg arc which allowed its position to be known to an accuracy of ±0.01 nm. For the calibration, the sample cuvette was replaced with a rough aluminum surface and the scattered laser excitation beam was focused into the spectrometer. The dye laser was scanned as usual through the nominal excitation range of 577–581 nm, and the output of the spectrometer photomultiplier was fed via an electrometer into the Nicolet. The resulting excitation spectrum showed a single line known to be 579.065 ± 0.010 nm. With use of this technique, the spectral width of the dye laser was found to be 0.06 nm, and the wavelength uncertainty of the excitation spectra should be no larger than twice the wavelength increments used to record the spectra which were always 0.019 nm.

Luminescence decay measurements were made using photon counting with an uncooled RCA 4832 photomultiplier. A PRA 1762/1763 amplifier/discriminator together with the Nicolet 1170 signal averager in pulse count mode were used for data acquisition. The bandwidth of this system was limited to 10 MHz by the Nicolet input amplifier so data were always collected at a count rate of 1 MHz or less to avoid distortion due to pulse pair resolution errors.

Results and Discussion

A. Characterization of Eu^{3+} Binding in Hemocyanin. The two lowest-energy multiplets associated with the $4f^6$ electronic configuration of Eu^{3+} are shown in Figure 1. Each energy level is labeled according to its $^{2s+1}L_j$ component which is then split by the ligand field; depending on the symmetry of the local environment, up to $2J + 1$ closely spaced components are possible. The Eu^{3+} ion luminescence spectra shown in Figure 2 are obtained by direct excitation of the metal ion at λ_{ex} of 465 nm for the $^7F_0 \rightarrow {}^5D_2$ transition. Curve A is the emission spectrum of Eu^{3+} in D_2O/Tris buffer at pH 7.0: the $^5D_0 \rightarrow {}^7F_1$ transition at 592 nm and the $^5D_0 \rightarrow {}^7F_2$ transition at 618 nm are observed to have moderately strong intensities while the $^5D_0 \rightarrow {}^7F_0$ transition at 579 nm is very weak. When Eu^{3+} binds to hemocyanin in the same buffer (curve B), the relative intensity of the $^5D_0 \rightarrow {}^7F_2$ transition changes dramatically due to the change in the ligand

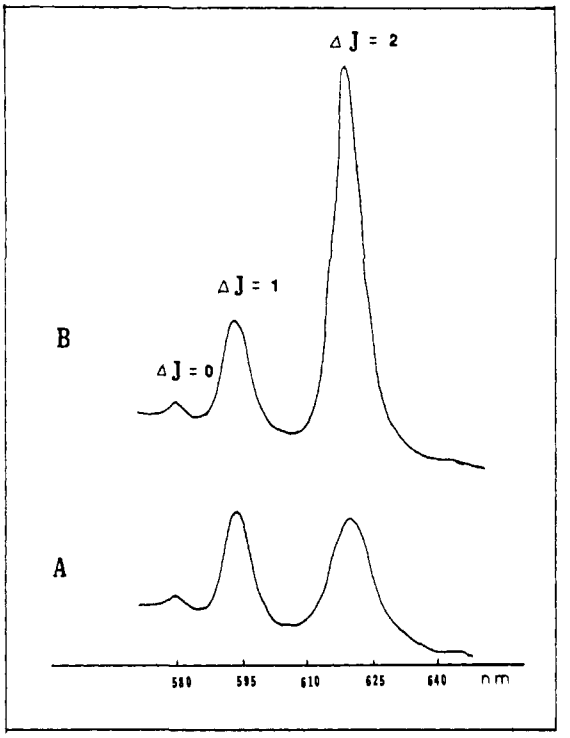

Figure 2. Emission spectra of (A) Eu^{3+} in D_2O/Tris buffer at pH 7.0 and (B) Eu^{3+} in oxyhemocyanin (D_2O/Tris buffer, pH 7.0). Eu^{3+} was excited at 465 nm. $\Delta J = 0$, 1 transitions are normalized to those in curve A, as these transitions are not sensitive to ligand environment.

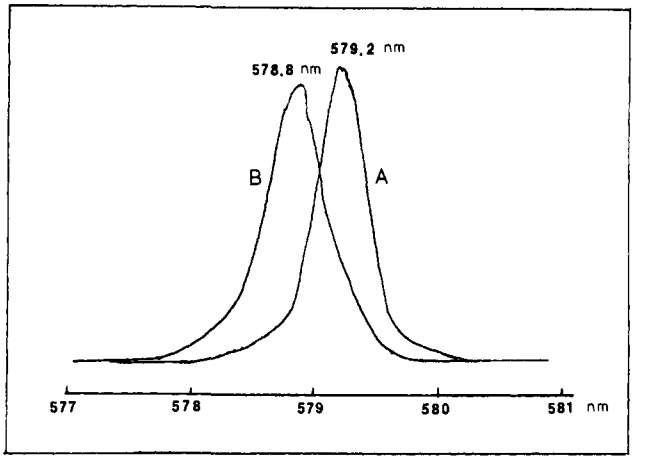

Figure 3. Excitation spectra of (A) Eu^{3+}–oxyhemocyanin in D_2O/Tris buffer, pH 7.0 (0.031 mM Eu^{3+}, 5 mM Tris, 0.075 oxy) and (B) Eu^{3+} in D_2O/Tris buffer, pH 7.0 (0.031 mM Eu^{3+}, 5 mM Tris). Emission monitored at 618 nm.

environment around the Eu^{3+} ion. This phenomenon is a reflection of the hypersensitive character associated with the $\Delta J = 2$ transition.[17] Although the $\Delta J = 2$ as well as $\Delta J = 1$ transitions have the advantage of possessing relatively high intensity, its ligand-field splitting (up to 5 components) complicates the spectrum. Thus, structural elucidation of Eu^{3+} binding utilizes the $^5D_0 \rightarrow {}^7F_0$ transition. As both the ground-state $^7F_0$ and the excited-state $^5D_0$ are nondegenerate, this transition must generate a single unsplit line for a given Eu^{3+} site. Since this transition energy is sensitive to the environment of Eu^{3+}, under sufficient resolution, this $^5D_0 \rightarrow {}^7F_0$ transition should provide an excellent diagnostic for probing the various types of Eu^{3+} coordination which may be present in the system. We can monitor the $^5D_0 \rightarrow {}^7F_2$ emission to obtain an excitation spectrum of the $^7F_0 \rightarrow {}^5D_0$ transition region. Ex-

(17) (a) Jørgensen, C. K.; Judd, B. R. *Mol. Phys.* **1964**, *8*, 281. (b) Chrysochoos, J.; Evers, A. *Chem. Phys. Lett.* **1973**, *18*, 115.

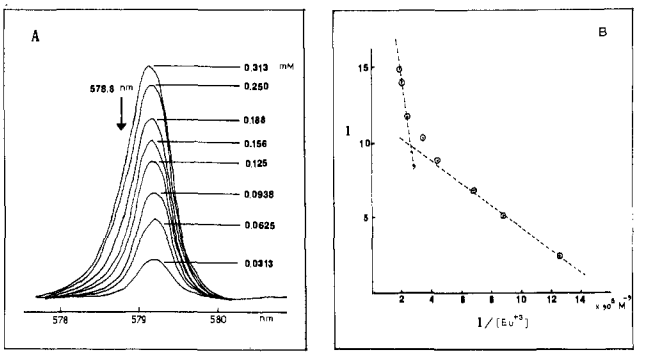

Figure 4. (A) Excitation spectra of Eu^{3+} titration of oxyhemocyanin in D_2O/Tris buffer, pH 7.0. (B) Plot of I vs. $I/[Eu^{3+}]$ for the Eu^{3+} titration of oxyhemocyanin in D_2O/Tris buffer, pH 7.0.

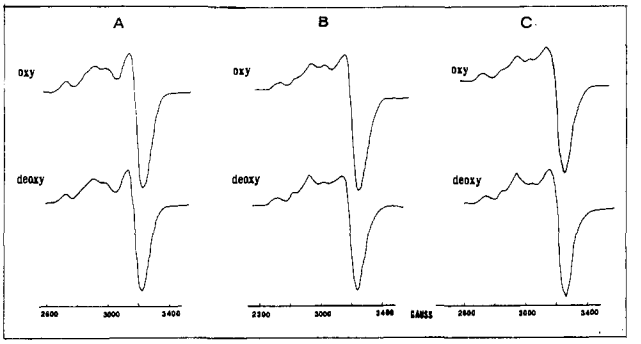

Figure 5. EPR spectra of *Busycon* Spectral Probe hemocyanin in 100-fold excess N_3^-: (A) oxy and deoxy without Ca^{2+}; (B) oxy and deoxy with 5 mM Ca^{2+}; (C) oxy and deoxy with 5 mM Eu^{3+}.

citation spectra of Eu^{3+} in deuterated Tris buffer at pH 7.0 with and without hemocyanin are distinctly different as shown in Figure 3. Eu^{3+}–hemocyanin (curve A) shows a sharp and intense peak at 579.2 nm while Eu^{3+}–Tris (curve B) shows a peak of comparable intensity centered at 578.8 nm. Thus, the excitation spectrum can be used to reliably identify Eu^{3+} bound to the protein. Although the sizable overlap of the hemocyanin-free and hemocyanin-bound Eu^{3+} spectra makes it difficult to quantitate accurately the binding properties of the Eu^{3+} ion, an estimate of the number of binding sites and the corresponding binding constants can be achieved by inspection of the Eu^{3+} titration behavior of hemocyanin. Lifetime studies indicate that Eu^{3+} in oxyhemocyanin has three lifetimes—τ_1, τ_2, and τ_3. As discussed in section C, all of the excitation spectra in the following study are gated at the τ_2 region.

In order to use Eu^{3+} titration as a probe of the binding properties of Eu^{3+} to hemocyanin, it is necessary to define the interaction of Eu^{3+} with Tris buffer in the absence of protein. At a concentration of 0.031 mM Eu^{3+}, the excitation spectrum shows a peak centered at 578.8 nm, whose intensity gradually increases as the Eu^{3+} concentration is increased. The maximum peak position shifts to lower energy (590.0 nm) after 0.34 mM of Eu^{3+} is added. This result suggests that more than one Eu^{3+}:Tris complex is formed in the titration procedure. However, if the Eu^{3+} concentration is kept below 0.25 mM, only one major Eu^{3+}–Tris component is present. Thus, in order to simplify the resultant spectra, the highest Eu^{3+} concentration in titrations of oxyhemocyanin was set to be 0.25 mM by lowering the oxyhemocyanin concentration.

Oxyhemocyanin, 0.078 mM in 5 mM Tris/D_2O buffer, was then titrated with Eu^{3+} resulting in the series of excitation spectrum shown in Figure 4. The intensity of the Eu^{3+} in this titration system ($Hc + Eu^{3+} \rightarrow Hc{\cdot}Eu^{3+}$) is then given by

$$I = \epsilon[Eu^{3+}] + \epsilon_1[Hc{\cdot}Eu^{3+}] \quad (1)$$

where ϵ and ϵ_1 are defined as the intensity at 579.2 nm of 1 mol of hemocyanin-free Eu^{3+} and 1 mol of hemocyanin–Eu^{3+}, respectively. Equation 1 can be rewritten as

$$I = \epsilon[Eu^{3+}] + \frac{[Hc_T]\epsilon_1 K_1[Eu^{3+}]}{1 + K_1[Eu^{3+}]} \quad (2)$$

where $[Hc_T]$ is the total hemocyanin concentration. The titration data presented in Figure 4A clearly demonstrate that the hemocyanin-free Eu^{3+} peak at 578.8 nm (as indicated by the arrow) grows in very slowly. Therefore, hemocyanin has a very high affinity for Eu^{3+} and, at low concentrations of Eu^{3+} (0.031 mM), most of the Eu^{3+} ions are bound. Thus, we consider the excitation spectrum shown in Figure 3, curve A, to represent the spectrum of a pure hemocyanin–Eu^{3+} complex. Using this Eu^{3+}–hemocyanin band shape as a standard, we are able to calculate the relative contribution of hemocyanin–Eu^{3+} at 578.8 nm and can then determine the concentration of hemocyanin-free Eu^{3+} in each of the spectra of Figure 4A. At low Eu^{3+} concentrations, the contribution of hemocyanin-free Eu^{3+} at 579.2 nm is negligible. Equation 2 may then be simplified and rearranged as

$$I = \epsilon_1[Hc_T] - \frac{I}{K_1[Eu^{3+}]} \quad (3)$$

The plot of I vs. $I/[Eu^{3+}]$ should give a straight line with a slope of $-1/K_1$.

A plot of I vs. $I/[Eu^{3+}]$ is shown in Figure 4**B**. The change in slope indicates at least two binding constants where we estimate $K_1 \simeq 10^5\ M^{-1}$ and $K_2 \simeq 10^4\ M^{-1}$. The titration data at higher Eu^{3+} concentrations cannot be obtained due to a reversible precipitation of protein which corresponds to a superaggregation of the hemocyanin biopolymer. Thus, the titration results demonstrate that at lower concentrations of Eu^{3+}, there are at least two specific types of binding sites per one binuclear copper site in hemocyanin, both with high Eu^{3+} affinity. When the Eu^{3+} concentration exceeds 4.5 × hemocyanin concentration, additional binding occurs, yielding the highly aggregated hemocyanin form.

B. Substitution of Eu^{3+} for Ca^{2+} in Hemocyanin. Although all of the chemical evidence described in the introduction strongly suggests that Eu^{3+} will substitute for Ca^{2+} in biological systems, we first provide results which demonstrate that Eu^{3+} occupies the Ca^{2+} site and performs the same allosteric role as Ca^{2+} does in native hemocyanin, before we attempt a detailed analysis of the Eu^{3+} binding site in hemocyanin. As the Spectral Probe biopolymers of hemocyanin[7] demonstrated an important role of Ca^{2+} in allosteric regulation of protein quaternary structure relating to oxygen binding, it should also probe a similar function for Eu^{3+}. When the *Busycon* Spectral Probe hemocyanin is treated with 5 mM Ca^{2+}, the half-met probe sites show a dramatic change in their EPR signal upon deoxygenation of the remaining oxy sites, due to the effects of site–site interaction induced by Ca^{2+} ions (Figure 5, parts A and B, see ref 7 for further discussion). Addition of 5 mM equiv of Eu^{3+} to the Ca^{2+}-free Spectral Probe hemocyanin shows a similar half-met EPR change upon deoxygenation (Figure 5C). The fact that Eu^{3+} affects oxygen binding in a way similar to that observed for Ca^{2+} is an indication that Eu^{3+} exhibits a heterotropic effector role parallel to that of Ca^{2+} in *Busycon* hemocyanin.

Further, competition between these two ions was carried out for binding to hemocyanin in Tris/D_2O buffer at pH 7.0. The excitation spectrum of 0.031 mM Eu^{3+} in the presence of oxyhemocyanin is shown in Figure 6, curve A. Successive addition of Ca^{2+} results in reduced intensity at 579.2 nm and the appearance of a shoulder at shorter wavelengths. As $[Ca^{2+}]$:$[Eu^{3+}]$ approaches 1000:1, the protein begins precipitating. At the end of the titration, the excitation spectrum of Eu^{3+} (Figure 6, curve E) is a mixture of hemocyanin-free and hemocyanin-bound Eu^{3+} and indicates that approximately one of the two Eu^{3+} ions is displaced by the binding site by the large excess of Ca^{2+}. This provides direct evidence that Ca^{2+} and Eu^{3+} do compete for the same binding site in hemocyanin. All of these results indicate that the Eu^{3+} is capable of both structurally and functionally substituting for Ca^{2+}. Therefore, the information we obtain on the Ca^{2+}-competitive Eu^{3+} binding site in hemocyanin in the

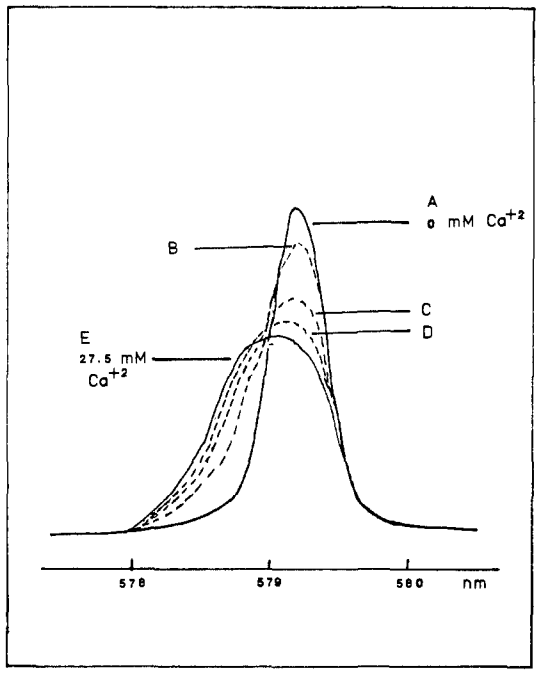

Figure 6. Excitation spectra of Ca^{2+} titration to Eu^{3+}–oxyhemocyanin (hemocyanin concentrations of 0.075 mM and Eu^{3+} concentration of 0.031 mM) in D_2O/Tris buffer, pH 7.0: (A) in the absence of Ca^{2+}; (B) with 5 mM Ca^{2+}; (C) with 10 mM Ca^{2+}; (D) with 15 mM Ca^{2+}; (E) with 27.5 mM Ca^{2+}.

following sections is appropriate for elucidating the structural characteristics of the corresponding Ca^{2+} binding site.

C. Effects of Deoxygenation of the Coupled Binuclear Copper Active Site on the Eu^{3+} Binding Site. The luminescence lifetime of the $^5D_0$ emitting state of Eu^{3+}, denoted by τ, can be expressed as rate constant k ($=1/\tau$), which can then be divided into four contributing terms:

$$k = k_H + k_r + k_{nr} + k_{ET} \quad (4)$$

where k_H is the radiationless rate constant for quenching via coupling to the O–H stretching vibration of the coordinated H_2O; k_r is the radiative rate constant for transition to the ground state; k_{nr} is the radiationless rate constant; and k_{ET} is the rate constant of Förster-type radiationless energy transfer which can be described by a through-space dipole–dipole mechanism. In hemocyanin, energy transfer may arise from dipole–dipole interaction between the Eu^{3+} chromophore and the binuclear copper-active site which exhibits intense absorption in the oxy form (ϵ_{570} 1000). Earlier work has established that a weak vibronic coupling between the Eu^{3+} excited state and the O–H oscillator of the coordinated water molecules leads to efficient deexcitation of the Eu^{3+} ion[18] and that the rate constant (k_H) is directly proportional to the number of O–H oscillators in the first coordination sphere.[19] In the case of D_2O, the deexcitation process via the O–D oscillator is much less efficient,[20] due primarily to the reduced vibrational frequency.

According to Hass and Stein,[20] only 4–5 vibrational quanta for H_2O, but 5–7 quanta for D_2O, must be excited in order to match the energy gap between the excited $^5D_0$ state and the ground multiplet state of the Eu^{3+} complex. The lower limit of the k_H/k_D ratio of about 200[21] allows one to assume that k_D is negligible compared to the other rate constants. Horrocks has performed experiments which demonstrate that this isotope effect allows a determination of the number of O–H oscillators in the first coordination sphere by carrying out experiments in H_2O and D_2O solutions.[15,16] In his study, a series of structurally characterized crystalline solids grown separately from D_2O and H_2O were used

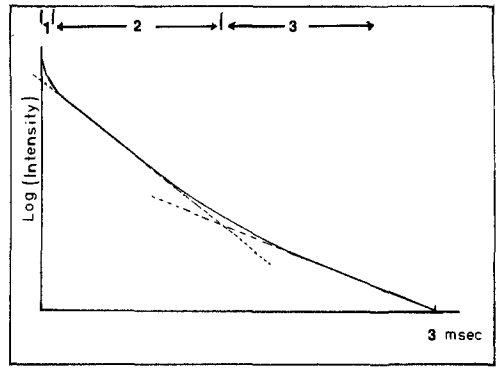

Figure 7. Log plot of the luminescence decay of Eu^{3+} in oxyhemocyanin in D_2O/Tris buffer, pH 7.0.

Table I. Lifetimes and Inner-Sphere-Coordinated Water Numbers of Eu^{3+} Binding Sites in Hemocyanin without Ca^{2+}

	lifetime, ms		coordinated water no.
	H_2O	D_2O	
oxy	0.12	0.42	6.5
deoxy	0.18	1.50	5.1
met			
oxygenated	0.14	0.93	6.2
deoxygenated	0.14	0.93	6.2

to establish the correlation between $\Delta\tau$ and the number of waters ($n/2$) in the first coordination sphere of the Eu^{3+} ion. Equation 5 describes the least-squares fit of the data points in the Eu^{3+} complexes[22,23]

$$n/2 = 1.05\left(\frac{1}{\tau_H} - \frac{1}{\tau_D}\right) \quad (5)$$

where τ_H and τ_D are the decay lifetimes of Eu^{3+} complexes in H_2O and D_2O, respectively. This correlation was also supported by the solution state data where a variety of Eu^{3+} chelating ligands were used to display the various number of water molecules from the first coordination sphere. We now employ this approach to the study of the hemocyanin–Eu^{3+} complex to probe the allosteric effects at the Ca^{2+} binding site induced by deoxygenation of the binuclear copper-active site.

A decay curve was obtained where 0.031 mM Eu^{3+} in oxyhemocyanin at pH 7.0, 5 mM Tris/D_2O buffer was excited at 579.2 nm ($\Delta J = 0$) and the emission intensity at 618 nm ($\Delta J = 2$) was recorded. The decay curve is then converted into a plot of log of relative fluorescence intensity vs. time (Figure 7), where the nonlinear behavior indicates the presence of more than one decay component in this system. In order to extract information from this system, we first divide the log plot into three regions as shown in Figure 7. The first region gives a very fast decay and contributes very litte in the log plot. In addition, all of the decay lifetime measurements in this study show that the fast component (τ_1) is insensitive to quaternary structure and to the nature of the binuclear copper of the different protein derivatives (i.e., oxy, deoxy, met). We therefore concentrate only on the second and the third regions. By assuming two decay lifetimes (τ_2 and τ_3), we fit the decay curve in regions 2 and 3 to eq 6,[24] where a is a

$$I(t) = a\exp(-t/\tau_2) + (1-a)\exp(-t/\tau_3) \quad (6)$$

constant of value less than 1. Curve fitting shows that the Eu^{3+} binding site with the shorter lifetime (τ_2) is the major component in the system ($a > 85\%$). We thus concentrate on understanding

(18) (a) Kropp, J. L.; Windsor, M. W. *J. Chem. Phys.* **1965**, *42*, 1599. (b) Kropp, J. L.; Windsor, M. W. *J. Phys. Chem.* **1967**, *71*, 477.
(19) Hass, Y.; Stein, G. *J. Phys. Chem.* **1971**, *75*, 3677.
(20) Hass, Y.; Stein, G. *J. Phys. Chem.* **1972**, *76*, 1093.
(21) Hass, Y.; Stein, G. *J. Phys. Chem.* **1971**, *75*, 3668.
(22) Rhee, M. J.; Sudnick, D. R.; Arkle, V. K.; Horrocks, W. Dew, Jr. *Biochemistry* **1981**, *20*, 3328.
(23) (a) Horrocks, W. Dew, Jr.; Collier, W. E. *J. Am. Chem. Soc.* **1981**, *103*, 2856. (b) Snyder, A. P.; Sudnick, D. R.; Arkle, V. K.; Horrocks, W. Dew, Jr. *Biochemistry* **1981**, *20*, 3334.
(24) Giunta, C., personal communication.

Table II. Lifetimes and Inner-Sphere-Coordinated Water Numbers of Eu^{3+} Binding Sites in Hemocyanin Saturated with 27.5 mM Ca^{2+}

	lifetime, ms		coordinated water no.
	H_2O	D_2O	
oxy	0.12	0.30	5.4
deoxy	0.18	1.20	5.0

the sites associated with τ_2. Table I lists the decay lifetimes (τ_2) for Eu^{3+}–oxyhemocyaninin H_2O/ and D_2O/Tris buffer. According to eq 5, the number of coordinated water molecules in the inner sphere of the Eu^{3+} is 6.5. As compared to the coordinated water number of 9.6 for Eu^{3+} in aqueous solution,[25] we conclude that when Eu^{3+} is bound to hemocyanin, there is a concomitant loss of ~3 molecules of water from the Eu^{3+} first coordination sphere indicative of coordination by ~3 protein groups. An analogous lifetime study was then conducted on Eu^{3+}–deoxyhemocyanin. Deoxygenation of the binuclear copper active site causes a dramatic increase of the Eu^{3+} lifetime (Table I). By use of eq 5, the number of coordinated water molecules in Eu^{3+}–deoxyhemocyanin is found to be 5.1, which is 1.4 ± 0.5 coordinated water molecules less than that of the oxygenated form. This result demonstrates a very important structural role of Ca^{2+}: as the protein goes from a relaxed to a tense quaternary conformation, Ca^{2+} releases at least one coordinated water molecule which likely results from binding additional protein ligands.

The lifetime of deoxy in D_2O buffer is larger than that observed for oxy in D_2O buffer (1.5 ms vs. 0.42 ms). This suggests that when the hemocyanin is deoxygenated, in addition to the elimination of the coordinated water molecules, further changes must take place at the Eu^{3+} binding site.

It is possible that the elimination of a water molecule on the hemocyanin-bound Eu^{3+} site, due to coordination of an additional protein ligand upon deoxygenation, could induce a rearrangement of the site geometry or add a high-frequency ligand vibration and affect the radiationless process (k_{nr} in eq 4). We are able to estimate the difference between the radiationless pathway for the oxy and deoxy quaternary structures by comparison of the decay rates of the met (vide infra) and deoxy in D_2O buffer. The Δk_{nr} is then calculated to be 0.41 ms^{-1}. Compared to the estimated quenching rate constant of O–H, ~1 ms^{-1},[18] this value of Δk_{nr} is too small to result from a nonexchangeable protein R–O–H ligand. Further, other possible protein ligands with C=O and C—O groups were found to have a small quenching rate constant (~0.04 ms^{-1}). Thus, it seems reasonable to attribute the change in k_{nr} between oxy and deoxy to a geometrical rearrangement of the Eu^{3+} binding site.

Similar lifetimes studies on the Ca^{2+} noncompetitive Eu^{3+} site have been performed to probe the possibility of allosteric effects on this extra Eu^{3+} site. The lifetimes of Eu^{3+} bound to oxy- and deoxyhemocyanins at this Eu^{3+} site in D_2O and H_2O buffers saturated with high concentration of Ca^{2+} are also reported in Table II. Two lifetimes are resolved by the curve-fitting procedure, with a small percentage of Eu^{3+} having a longer lifetime. As before, we were interested in the major component, which has a lifetime somewhat different from that measured for Eu^{3+} in the absence of Ca^{2+}. According to eq 5, the coordinated water number is 5.4 in oxyhemocyanin and 5.0 in deoxyhemocyanin, which are within estimated uncertainty[16] of ±0.5 water molecule for eq 5. Hence, the lifetimes, in the absence of Ca^{2+}, listed in Table I derive from a combination of two unresolvable Eu^{3+} decays. Consequently, the calculated water number change is an average for these two sites, and the actual change of lifetime as well as coordinated water number for the Ca^{2+} competitive site should be somewhat larger than that listed in Table I.

D. Estimation of the Distance between the Coupled Binuclear Copper-Active Site and the Allosteric Ca^{2+} by Internal Energy Transfer. The decay rate constant for Eu^{3+} bound to oxyhemocyanin in D_2O buffer can be expressed as

$$k_{oxy}(D_2O) = k_{r(oxy)} + k_{nr(oxy)} + k_{ET(oxy)} \quad (7)$$

k_{ET} specifically deals with Förster type energy transfer between Eu^{3+} and the copper-active site, which is highly dependent on the spectral overlap integral, J, defined by eq 8,[26] where $F(\nu)$ is the

$$J = \frac{\int F(\nu)\epsilon(\nu)\nu^{-4}\,d\nu}{\int F(\nu)\,d\nu} \quad (8)$$

luminescence intensity of Eu^{3+} complex, $\epsilon(\nu)$ is the molar extinction coefficient of the copper-active site, and ν is the frequency in cm^{-1}. As deoxyhemocyanin does not have any absorption features in the 580- to 620-nm region of the optical spectrum, the spectral overlap integral, J, equals zero and therefore the possibility of radiationless energy transfer of Eu^{3+} to the deoxy copper-active site does not exist. The decay rate constant of Eu^{3+} bound to deoxyhemocyanin is then expressed as

$$k_{deoxy}(D_2O) = k_{r(deoxy)} + k_{nr(deoxy)} \quad (9)$$

Equations 7 and 9 indicate that the change of lifetime between oxy and deoxy in D_2O buffer contains contributions due to energy transfer from the Eu^{3+} site to the oxy site. However, as mentioned previously, this comparison is complicated by the changes in τ_{nr} due to coordination of an additional protein ligand and its concomitant geometry change at the Eu^{3+} binding site in the deoxy tense quaternary structure. Alternatively, the met derivative, in which the exogenous peroxide ligand in oxyhemocyanin is replaced by water eliminating the absorption features in the 580-nm region which would be responsible for quenching the Eu^{3+} emission, is ideally suited for this comparison. First, all of our chemical and spectroscopic studies[1,27] have demonstrated strong active-site structural similarity between met and oxy. Second, a hemocyanin derivative can be prepared where various amounts of the met derivative are dispersed homogeneously into the oxy biopolymer.[28] As the percentage of the met derivative increases, the remaining oxyhemocyanin yields an oxygen-binding curve which shifts further toward the relaxed state with a P_{50} lower than that of pure oxyhemocyanin. Finally, while lifetime analyses show that Eu^{3+}–methemocyanin has a lifetime of 0.14 ms in H_2O buffer and 0.93 ms in D_2O buffer (Table I), the coordinated water number is determined to be 6.2, within experimental error of that of Eu^{3+}–oxyhemocyanin (6.5). These observations suggest that the met derivative may be viewed parallel to oxy as having a relaxed quaternary structure. Thus, the marked difference between the lifetime of Eu^{3+} bound to oxyhemocyanin (0.42 msec) and methemocyanin (0.93 msec) in D_2O buffer should be attributable to energy transfer from the Eu^{3+} site to the oxyhemocyanin coupled binuclear copper-active site.

As radiationless energy transfer has been used to estimate distances between metal ion chromophores and metal ion acceptors,[29,30] results for Eu^{3+} bound to the met derivative enable us to calculate the distance between the copper-active site and the allosteric Ca^{2+} site by monitoring the energy transfer in the oxy form. According to Förster,[31] the efficiency of dipole–dipole energy transfer, E, depends on the actual distance (r) between the donor and acceptor, which can be expressed as

$$E = \left[1 + \left(\frac{r}{R_0}\right)^6\right]^{-1} \quad (10)$$

R_0 is the critical distance for 50% energy transfer, which is given by

(25) Rhee, M. J.; Horrock, W. Dew, Jr.; Kosow, D. P. *Biochemistry* **1982**, *21*, 4524.

(26) Förster, T. *Ann. Phys.* **1948**, *2*, 55.

(27) Himmelwright, R. S.; Eickman, N. C.; LuBien, C. D.; Solomon, E. I. *J. Am. Chem. Soc.* **1980**, *102*, 5378.

(28) Hwang, Y. T.; Bonaventura, C.; Solomon, E. I., unpublished results.

(29) Berner, V. G.; Darnall, D. W.; Birnbaum, E. R. *Biochem. Biophys. Res. Commun.* **1975**, *66*, 763.

(30) Horrocks, W. Dew, Jr.; Holmquist, B.; Vallee, B. L. *Proc. Natal. Acad. Sci. U.S.A.* **1973**, *72*, 4764.

(31) Förster, T. In "Quantum Chemistry"; Sinanoglu, O., Ed.; Academic Press: New York, 1965; Part III.

$$R_0^6 = (8.78 \times 10^{-25})k^2\Phi n^{-4}J \quad (11)$$

A value of 1.36 is taken for the refractive index, n, which is intermediate between that of water (1.33) and that of organic molecules composed of first-row atoms (1.39).[23] The orientation factor, k^2, is set equal to $^2/_3$ assuming an isotropic donor and acceptor. To determine the quantum yield, Φ, of the Eu^{3+} chromophore, we employ the relationship given in eq 12, where

$$\frac{\Phi_A}{\Phi_B} = \frac{k_{r,A}\tau_A}{k_{r,B}\tau_B} \quad (12)$$

Φ_A, $k_{r,A}$, τ_A, Φ_B, $r_{r,B}$, and τ_B denote the values of these quantities for chromophores A and B, respectively. Assuming that k_r is not protein dependent, we can estimate the quantum yield for Eu^{3+} in the met derivative by substituting reported values of τ and Φ into eq 12. Horrocks indicates that Eu^{3+} bound to thermolysin has a lifetime of 0.56 ms and a quantum yield of 0.27 in H_2O.[23] Although quantum yields are difficult to measure with accuracy, the value for Eu^{3+} bound to thermolysin is independently corroborated by an energy transfer distance measurement which agrees with the crystallographically derived distance.[23] By substituting these values into eq 12, we then estimate $\Phi_{Eu} = 0.0675$ in H_2O for our system. The spectral overlap integral, J, can be calculated from the emission spectrum of Eu^{3+} in the protein and the absorption spectrum of oxyhemocyanin in the region of the Eu^{3+} luminescence. The resultant J value is 1.8×10^{-14} cm^6 mol^{-1}. This J value, along with the estimated values of other parameters, estimates $R_0 = 24.7$ Å in H_2O buffer. As the Förster type radiationless energy transfer affects both the observed luminescence intensity, I, and the excited-state lifetime, τ, of the donor, the efficiency of energy transfer can also be expressed as

$$E = 1 - \frac{I}{I_0} = 1 - \frac{\tau}{\tau_0} \quad (13)$$

I_0, τ_0 and I, τ denote the values of the quantities in the absence and presence of energy transfer. Combining eq 10 and 13 we have

$$1 - \frac{\tau}{\tau_0} = \left[1 + \left(\frac{r}{R_0}\right)^6\right]^{-1} \quad (14)$$

From this equation, the average distance (r) between the hemocyanin copper-active site and the Eu^{3+} allosteric site is estimated to be 32.8 Å. Analogous calculation in D_2O buffer ($r = 32.3$ Å) confirms this result.

E. Oxygen Effects on the Eu^{3+} Fluorescence. It has been shown that dissolved oxygen efficiently quenches fluorescence in many systems.[32] To test this quenching effect in the hemocyanin system, decay lifetimes were measured for 2.5 mM Eu^{3+} in D_2O/Tris buffer saturated with air and Ar, respectively. The observed decay lifetimes are identical for these two solutions (0.44 ms), which shows that the bimolecular collision between O_2 and Eu^{3+} makes no contribution to the fluorescence quenching of Eu^{3+} in solution. However, Kuiper et al.[33,34] have replaced Ca^{2+} by terbium in *Panulixus interruptus* hemocyanin and reported that addition of O_2 to Tb^{3+}-saturated apohemocyanin decreased the Tb^{3+} fluorescence intensity. Accordingly, they suggest that O_2 is an effective quencher of the emission of the protein-bound Tb^{3+}. Since in his experiment Tb^{3+} emission was sensitized by the tryptophan amino acid residues, it is possible that O_2 has quenched the tryptophan instead of the Tb^{3+} emission. In our study, Eu^{3+} was substituted for Ca^{2+} and excited directly into the intraconfiguration f–f transition by a laser source. The simplicity of this system eliminates the possibility of sensitizer quenching. In order to investigate the effect of oxygen on protein-bound Eu^{3}, we extended this study to the effect of O_2 on met derivative. As the met active site derivative does not react with the oxygen, its addition to a deoxygenated met solution can neither induce protein conformational change nor Förster type energy transfer. Thus, the met derivative in D_2O buffer was saturated with Ar and air, separately, and the lifetimes were measured. No change in lifetime was observed (see Table I). This demonstrates that dissolved oxygen has no effect on the protein-bound Eu^{3+} fluorescence. Therefore, the lifetime difference observed between oxy- and deoxyhemocyanins is completely due to the effects of oxygen binding to the coupled binuclear copper-active site.

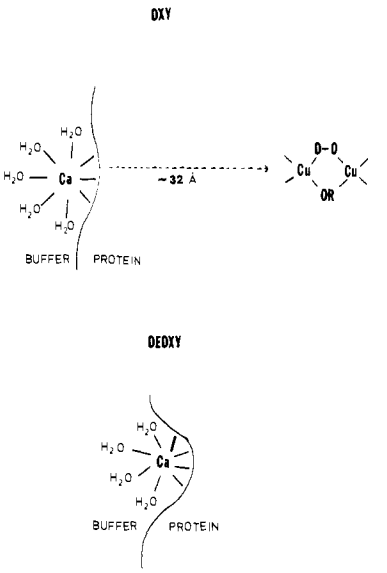

Figure 8. Preliminary models for the allosteric Ca^{2+} binding site in the relaxed (oxy) and the tense (deoxy) quaternary structures. (Note that the distance to the coupled binuclear copper-active site could not be estimated for the deoxy quaternary structure due to the lack of Förster energy transfer.)

Summary

At this point, we have determined that the addition of Eu^{3+} to the hemocyanin biopolymer results in two kinds of binding. One correlates to the allosteric Ca^{2+} binding site, which is closely linked to the conformational change induced by oxygen binding at the binuclear copper active site. The second Eu^{3+} is Ca^{2+} noncompetitive and is not associated with the biological function of the hemocyanin. Our results suggest that the Ca^{2+} site is located in a very hydrophilic environment at a distance of ~32 Å from the binuclear copper-active site.

In the relaxed quaternary structure there appears to be ~3 protein ligands and ~5 H_2O molecules binding to Ca^{2+}. Deoxygenation of the coupled binuclear copper-active site produces a tense protein quaternary structure which results in loss of ~1 water at the Ca^{2+} binding site. This likely relates to the coordination of an additional protein ligand to the Ca^{2+} ion (Figure 8) and correlates to the role of this ion in stabilizing the tense quaternary structure of the hemocyanin biopolymer.

Registry No. Calcium, 7440-70-2; oxygen, 7782-44-7; copper, 7440-50-8; europium, 7440-53-1.

(32) Eininger, J.; Lamolo, A. A. *Biochem. Biophys. Acta* **1971**, *240*, 299.
(33) Kuiper, H. A.; Zalla, L.; Finazzi-Argo, A. *J. Mol. Biol.* **1981**, *149*, 805.
(34) Kuiper, H. A.; Finazzi-Agro, A.; Antonini, E.; Brunori, M. *FEBS Lett.* **1979**, *99*, 317.